Front. Earth Sci. 2016, 10(1): 183–194
DOI 10.1007/s11707-015-0501-z

RESEARCH ARTICLE

Ground-penetrating radar study of beach-ridge deposits in Huangqihai Lake, North China: the imprint of washover processes

Xin SHAN[1,2], Xinghe YU (✉)[1], Peter D. CLIFT[2], Chengpeng TAN[1], Shunli LI[1], Zhixing WANG[1], Dongxu SU[1]

1 School of Energy Resources, China University of Geosciences (Beijing), Beijing 100083, China
2 Department of Geology and Geophysics, Louisiana State University, Baton Rouge, LA 70803, USA

Abstract Determining the origin of beach ridges in lacustrine basins can often be problematic. The sedimentary processes responsible for formation of beach ridges on the north shore of Huangqihai Lake were investigated by using ground penetrating radar (GPR). A 400 MHz GPR antenna was used to achieve a high vertical resolution of 0.04–0.08 m. The radar stratigraphy was then determined using principles of seismic stratigraphy. The radar facies (RF) were determined by analyzing internal configuration and continuity of reflections, as well as reflection termination patterns.

The identified RF fall into three groups (inclined, horizontal and irregular). The inclined group consists of RF that display inclined reflections. The horizontal group consists of RF that exhibit predominantly horizontal reflections. In the irregular group, the reflections are typically weak. RF with reflections with gently landward dips in the shore-normal profile are interpreted as washover sheet deposits. RF with steeply landward-dipping and imbricated reflections are interpreted as washover lobes. Washover sheets develop when overwash fails to enter a significant body of water and sedimentation takes place entirely on the relatively flattened topography. Washover lobe development occurs when overwash enters a region in which topography dips steeply landward, and sedimentation takes place on the surface of washover sheets or previous washover lobes. The beach-ridge deposits are interpreted as being formed entirely from vertically and laterally stacked washover sheets and washover lobes. They were formed by wave-dominated processes and secondary overwash processes supplemented by longshore currents.

Received August 10, 2014; accepted October 8, 2014

E-mail: billyu@cugb.edu.cn

Keywords beach-ridge, ground penetrating radar, radar facies, radar stratigraphy, washover process

1 Introduction

Beach ridge systems have long been identified as components of lacustrine coastal depositional environments (Drake and Bristow, 2006; Harvey, 2006; Nichols, 2009; Leeder, 2011). Sedimentary rocks formed from beach ridges commonly serve as good hydrocarbon reservoirs between lacustrine basin shales (Deng et al., 2011; Jiang et al., 2011). Many characteristics of lacustrine deltas, ridges, beaches and deep-water deposits are similar to those from marine environments because many of the processes operating in the two environments are similar (Scholz et al., 1990; Best et al., 2003; Yu et al., 2012). Beach ridge systems are often categorized as being relict, semiparallel, multiple, wave or wind-built landforms (Otvos, 2000). Beach ridge systems essentially reflect the interaction between the supply of sediment and basinal reworking processes. Waves give rise to a variety of currents, which are directed offshore (rip currents), parallel with the shore (longshore currents) and onshore (onshore residual motions) (Nichols, 2009; Leeder, 2011). Shoreline profiles have a number of zones, each with characteristic processes, morphology and facies (Talbot and Allen, 1996). The beach-ridge system on the north shore of Huangqihai Lake was formed at the landward limit of wave penetration, namely in the swash zone. This study of beach ridges is designed to aid in the recognition of paleo-beach ridges elsewhere and to improve understanding of the processes responsible for their formation in lacustrine settings.

For decades techniques such as geophysical logging, seismic tests, ground-penetrating radar (GPR), and examination of outcrops have been used to study the

sedimentary characteristics and architectural elements of marine beach ridge systems (Anthony, 1995; Nielsen and Clemmensen, 2009). However, lacustrine beach ridge systems have received little detailed research. Important advances in our understanding of their internal structure has developed recently by application of GPR, which has been widely used to document the nature of fluvial and deltaic deposits (Corbeanu et al., 2001; Best et al., 2003; Lee et al., 2007). Based on analysis of GPR profiles in the beach-ridge system, it is possible to document and identify different types of washover deposits in such systems in Huangqihai Lake.

This paper presents a case study of a relict beach-ridge system. The objectives are to (i) document the radar stratigraphy and radar facies of the beach ridge, (ii) analyze the sedimentary origin of different radar facies, and (iii) describe sedimentary processes that are responsible for formation of the beach ridge to the north of Huangqihai Lake.

2 Geological setting

Huangqihai Lake in North China is roughly triangular in shape (Fig. 1(a)) and is elongate with a water depth of only 10 m due to the arid climate (Fig. 1(b)). Huangqihai Lake is 17.5 km long and 9 km wide with an area of 110 km^2. The lake is in a hydrologically closed basin fed by 19 rivers and streams including the Quanyulin, Mozishan, and Bawanghe Rivers. It is located at the transition between semi-humid and semi-arid areas in the middle temperate zone of China (Zhang et al., 2011). In summer, the lake area is dominated by southeasterly wind, contrasting with northwesterly wind in winter. The supply of sediment is often seasonally controlled. In summer, the sediments are transported mainly by rivers while in the winter the lake receives little influx. In the past decades, most of the rivers have been intermittent or even dry as a result of human impact and climate aridification.

The beach ridge system developed in the foreshore area, which is in the swash zone on the northern shore of the lake. Sand and gravel are supplied to the foreshore zone and are derived from the surrounding mountains which comprise Tertiary basalt, igneous rock and Quaternary clastic sediments. The beach ridge deposits are mainly medium-coarse grained sands with a matrix of clay, silt and subrounded-subangular granules. The potential source of northern beach ridge system was the northern igneous mountains. The beach ridge system exists in an area where the gradient of the depositional coastlines is less than 2°.

The beach ridge system on the northern shore of Huangqihai Lake is about 1 km length and 150–175 m wide (Fig. 1(c)). The shape of the beach ridge system is gently curved and its long axis is parallel with the paleo-shoreline (Fig. 1). However the lake level has fallen dramatically as a result of the dry climate and human impact during the past decades. The beach ridge system is now above the lake level (Figs. 1(b) and 1(d)). The top of the beach ridge system has been altered by eolian processes and bioturbation by shrubs and grasses. The beach ridge system generally trends northwest-southeast and is up to 1.6 m thick.

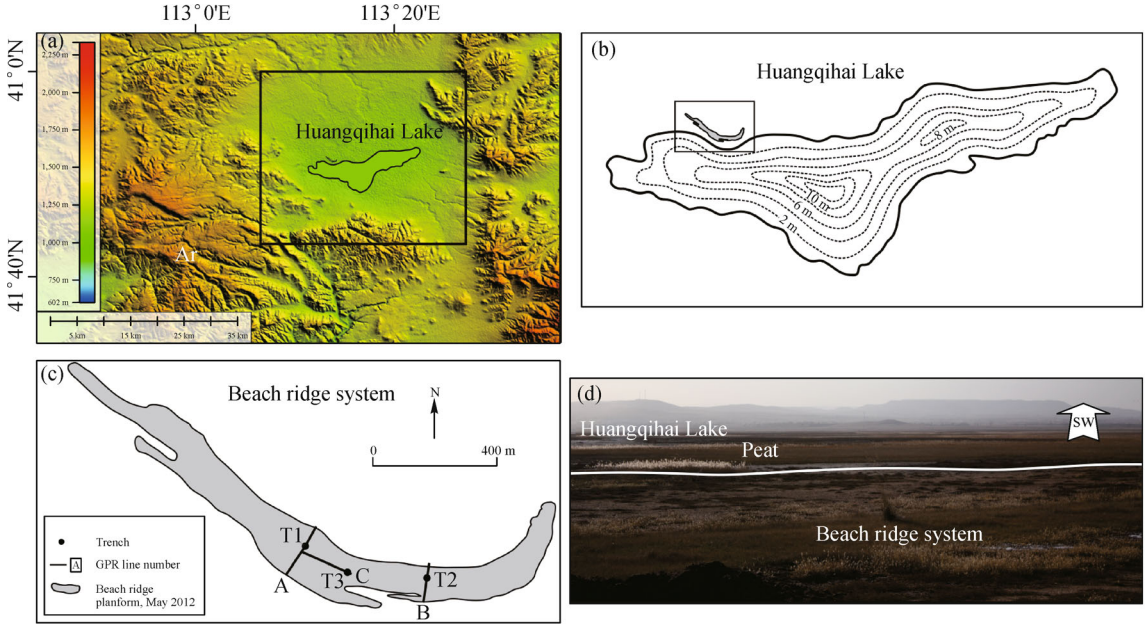

Fig. 1 Study site and location. (a) A GMT topographic map with the Huangqihai area highlighted within a square. Data is from SRTM (Shuttle Radar Monitoring Mission). (b) Bathymetry map of the dried out Huangqihai Lake in May, 2012. Depths were mapped by GPS as part of this study. (c) Planform map of the study beach ridge system in May 2012 with the locations of the 400 MHz GPR profiles and Trenches T1, T2 and T3. (d) Aerial photograph in May 2012 of the beach ridge system taken from the north.

3 Materials and methods

The GPR measurements involved deployment of a transmitter and a receiver in a fixed geometric pattern. The devices were moved over the surface to detect reflections from subsurface features. The method uses electromagnetic waves emitted from a transmitter to probe the subsurface. When these waves encounter changes in dielectric properties under the ground, some waves are reflected back to the receiver. The signal is then recorded and processed. Subsurface materials are often described as dielectrics, with the parameters permittivity and conductivity termed as dielectric properties. The electrical parameters of dielectrics are determined by: 1) water saturation, 2) the type of water (whether the water was saline or fresh), 3) mineralogical changes, for instance sand, shale, limestone or soil, and 4) porosity.

The subsurface deposits of the beach ridge system were surveyed using a TerraSIRch SIR 3000 system produced by Geophysical Survey Systems, Inc. (GSSI). The antenna frequency controls the depth of penetration and image resolution. The trial survey showed the 400 MHz antenna provided optimal resolution and penetration depth (up to 2.5 m). Below that depth muddy substrate and water intrusion caused rapid attenuation of the radar signal. Furthermore, the thickness of the beach-ridge system is about 1.6 m. The vertical resolution is 0.04–0.08 m.

The survey was obtained using a network of intersecting transects that capture the extent and variability of GPR reflections. The profiles were arranged parallel and perpendicular to the long axis (west to east) of the beach ridge (Fig. 1). In this study, three profiles (two shore-normal and the other one shore-parallel) were selected to illustrate the radar stratigraphy, radar facies and origin of the beach-ridge deposits.

Reflexw Software developed by Sandmeier Scientific Software company was used for editing and processing the GPR data. Basic GPR data processing involved five steps. 1) The raw data quality was good and data editing is the first task in the processing sequence. 2) Dewowing is the second step to reduce the data to a mean zero level and allow positive-negative colour filling to be used in the traces. 3) After data editing and dewowing, traces require adjustment to a common time-zero position before processing methods can be applied. Because the quality of the data was very good, filtering was not necessary. 4) The previous steps have operated in the time domain and the data was converted to depth. In order to convert time to depth, subsurface velocity must be known. The velocity was calculated from Common Mid-Point (CMP) analysis. The velocity profile was imported from CMP analysis and sections were then converted to a depth scale. In practice, CMP analysis tends to produce approximate velocity values with errors and variance of $\pm 10\%$ or worse. A velocity of 0.09 m/ns has been calculated from the CMP survey conducted at a depth of 40 cm in the beach ridge deposits. These results are consistent with published velocities for dry sands (Jol and Bristow, 2003). 5) Finally, the elevation is corrected for the effects of topography.

To link the GPR results with sedimentary layers, trenches were dug at selected positions along the GPR profiles (Fig. 1). A total of three trenches (about 1.5 m long, 1 m wide and ~1.5 m deep) were excavated using shovels and hoes. The trenches were selected to show characteristics of the washover deposits and the relationship between radar surfaces and the surfaces of sedimentary units.

3.1 Radar stratigraphy

Radar stratigraphy can be defined as the study of stratigraphy and depositional facies as interpreted from GPR data using seismic stratigraphy principles (Bristow, 2009). Radar stratigraphy provides higher resolution compared with seismic stratigraphy. The radar stratigraphic framework divides the radar profile into units, which represent different periods of sedimentation. Each single unit may be interpreted as a conformable and genetically related episode of sedimentation. As a result the boundary between units observed in the radar stratigraphy often separates sedimentary units of different origin. Considering the resolution of the GPR data, the radar stratigraphy or the boundaries between radar facies (RF) corresponds to the 3rd-order rank sedimentary boundaries using Miall's (1988) classification of depositional units. Depositional environments can thus be inferred through an orderly approach to the interpretation of GPR reflections.

The identification of termination patterns is important for constructing a relative chronology because terminations or boundaries represent chronostratigraphic gaps. The relative chronology of successive radar sequences can be deduced by laws of superposition and cross-cutting relations (Neal et al., 2003). As a result the radar stratigraphy often separates two different radar facies (RF), which have different termination patterns and reflections.

3.2 Radar facies

A radar facies is a mappable, 3D sedimentary unit composed of GPR reflections whose parameters differ from adjacent units (Jol and Bristow, 2003). Radar facies provides a way of classifying reflection character and subdividing GPR profiles into units that are formed by different sedimentary processes. Varying degrees of textural and compositional heterogeneity of sediments produce dielectrical contrasts, which generate subsurface reflections. Radar facies have been proven to compare well with sedimentary facies. Each package of radar facies was defined as a 3D sedimentary mass rather than as a 2-D reflection pattern in order to deduce the direction of

progradation and aggradation from inclined reflections.

Characteristics of radar facies were interpreted based on the internal configuration and continuity of reflections, as well as reflection termination patterns. The interpretation of radar facies and stratigraphy is derived from methods of seismic facies analysis. In turn, radar stratigraphy is the basis of investigating geometry and the relationships between different depositional packages. Reflection patterns are related to the lithologic and stratigraphic characteristics of sediments.

4 Results

4.1 Radar stratigraphy and radar facies of GPR profiles

The GPR profiles are described in terms of radar stratigraphy and facies following the principles outlined and suggested by Neal et al. (2002) and Neal (2004). Three GPR sections (Profiles A and B, which are shore-normal, and Profile C which is shore-parallel) covering the beach-ridge were selected for detailed analysis.

Based on identification of reflection terminations, it is possible to apply the principles of radar stratigraphy. Most radar surfaces terminate against each other (e.g., A-c against A-b, etc.).

4.1.1 Profile A

Nine radar facies (A-1−A-9) with different radar reflection characteristics were separated by identified radar surfaces (Fig. 2). Profile A is a shore-normal profile located in the west portion of the beach ridge system and is about 80 m long. The continuous, gently undulating boundary surface A-a marks the base of the radar stratigraphy. Radar facies A-1 underlies Surface A-a. Facies A-1 is characterized by horizontal reflections. The low amplitude was interpreted as being the product of weak dielectric contrasts between the sediments and could reflect a relatively homogeneous lithology. Weak reflections are typical of, but not necessarily unique to marsh peat deposits. Radar facies A-1 is interpreted to represent beach deposits, which were influenced by wave processes. The same reflection pattern has often been interpreted as beach deposits in similar settings (Tamura et al., 2008; Bennett et al., 2009).

Above Surface A-a, eight radar facies were delineated by radar surfaces and characterized by their different reflection characteristics and termination patterns (Table 1). Reflections within radar facies A-2 are discontinuous and sub-horizontal. To landward, radar facies A-2 and A-3 are bounded by Surface A-c. Radar facies A-4 is characterized by gently landward dipping, stacked and lenticular sediment sheets. It is bounded by Surfaces A-b and A-d and has similar characteristics as radar facies A-3. Radar facies A-8 is bounded by Surfaces A-g and A-h and is characterized by gently landward dipping reflections. Radar facies A-2, A-3, A-4 and A-8 are all characterized by gently landward-dipping (no more than 5°), discontinuous and stacked reflections (Fig. 2). They are interpreted as washover sheet deposits.

Radar facies A-5 and A-7 are dominated by steeply landward-dipping reflections, which show downlap on radar Surface A-d. Internally these facies are characterized by discontinuous and moderately strong amplitude reflections. Surfaces overlying radar facies A-5 and A-7 show erosional truncation, and are interpreted as boundaries representing periods of minor erosion. Radar facies A-6 is bounded by Surfaces A-f and A-h and is characterized by lakeward dipping, discontinuous and middle-strong amplitude reflections. Radar facies A-5 and A-7 are characterized by steeply landward-dipping, discontinuous, imbricated stacking patterns, which are interpreted as washover lobes.

Radar facies A-6 is interpreted as the product of wave processes acting on original beach-ridge deposits. The thickness of this unit varies from 0.1 to 0.4 m and appears thickest directly below the beach-ridge crest. Radar facies A-6 is interpreted either as swash lamination due to the dominance of a strong swash process, or washover sheet deposits.

Radar Facies A-9 is bounded by Surface A-h as its lower boundary and has the characteristics of high amplitude, continuous and stable reflections. This surface is the product of air wave and ground wave (system noise).

Trench 1, which is located in the middle of Profile A, shows a good correspondence between sedimentary units and radar facies (Figs. 2 and 3). Radar Surfaces A-b, A-d, A-e, A-f and A-h correspond well to surfaces between different lithology. Radar facies A-7 is characterized by slightly gravelly sands, which show a low textural maturity. The large scale landward-dipping planar bedding of radar facies A-5 and A-7 is interpreted to be the product of the action of washover processes on earlier deposits. In contrast, the roughly sub-horizontal reflections within Radar facies A-2 are interpreted as representing washover sheets welded onto the previous beach deposits (Radar facies A-1). Radar facies A-9 is a gravelly immature soil.

4.1.2 Profile B

Profile B, like Profile A is also shore-normal and lies in the eastern portion of the beach ridge system. The length of Profile B is 85 m. Seven Radar facies (B-1 to B-8) with different radar reflection characteristics were separated by radar surfaces (Fig. 4). Below Surface B-a, Radar facies B-a is interpreted as beach deposits. Above Surface B-a, seven radar facies were delineated by radar surfaces (Table 2). Radar facies B-2 and B-3 are high-amplitude, sub-continuous and steeply landward-dipping reflections, which are interpreted as washover lobe deposits. To

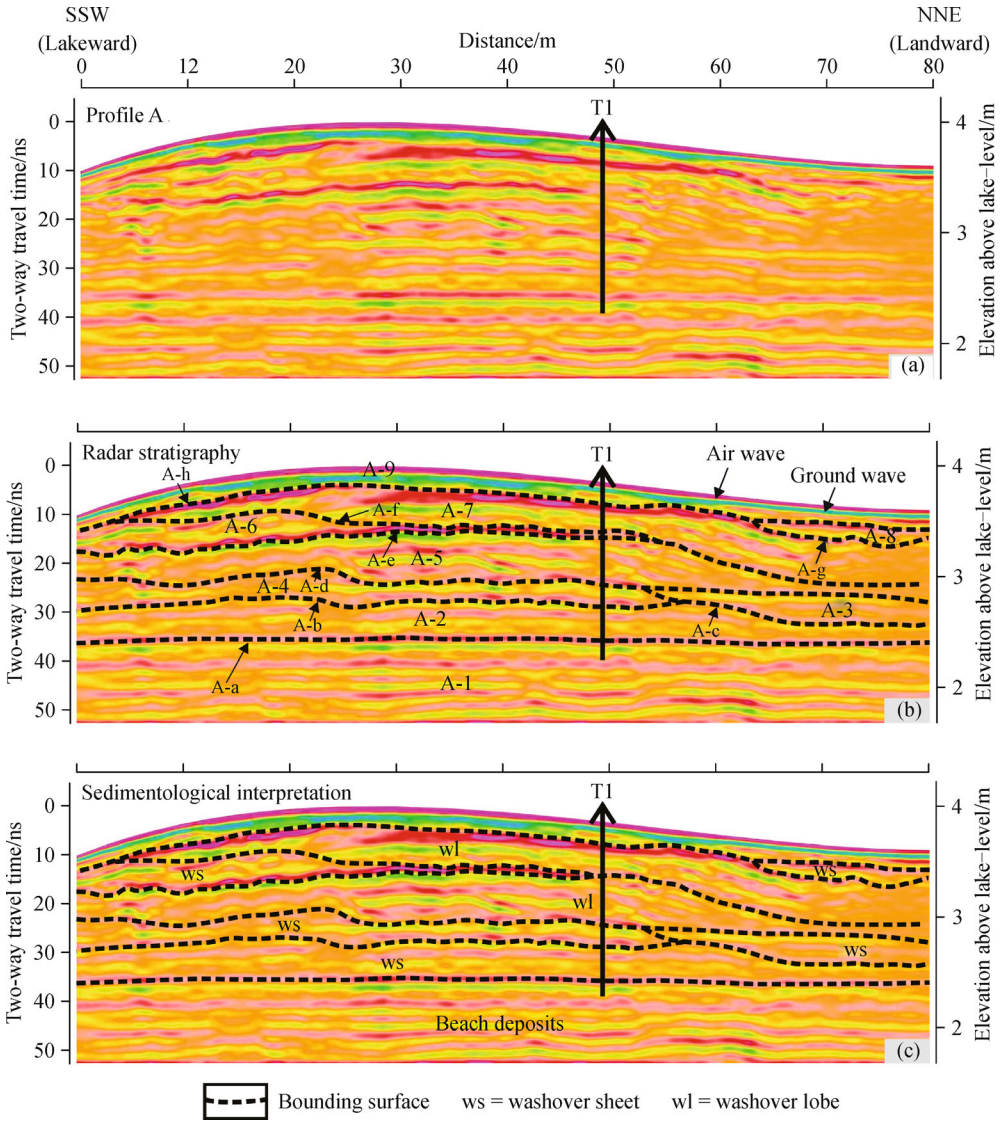

Fig. 2 A 400 MHz GPR survey collected by a TerraSIRch SIR 3000 (profile A; 80 m length) with (a) the processed GPR profile, (b) the subsurface radar stratigraphy based on the GPR data, and (c) the sedimentological interpretation based on internal reflection characteristics. The dashed lines represent boundaries between different radar facies. ws = washover sheet, wl = washover lobe. T1 shows the location of Trench 1.

Table 1 Characteristics of reflections of different radar facies within Profile A.

RF	Radar surface	Sedimentary origin	Dip	Continuity	Amplitude
A1	A-a	Beach deposits	Gently landward-dipping	Continuous	Middle
A2	A-a, A-b , A-c	Washover sheet	Gently landward-dipping	Discontinuous	Low-middle
A3	A-c, A-d	Washover sheet	Gently landward-dipping	Discontinuous	Low-middle
A4	A-b, A-c, A-d	Washover sheet	Gently landward-dipping	Discontinuous	Low-middle
A5	A-d, A-e	Washover lobe	Steeply landward-dipping	Discontinuous	Middle
A6	A-e , A-f, A-h	Washover sheet or swash lamination?	Lakeward-dipping	Discontinuous	Middle
A7	A-f, A-h	Washover lobe	Steeply landward-dipping	Discontinuous	Middle-high
A8	A-g, A-h	Washover sheet	Gently landward-dipping	Discontinuous	Middle
A9	A-h	Soil	? (System noise)	Continuous	Middle-high

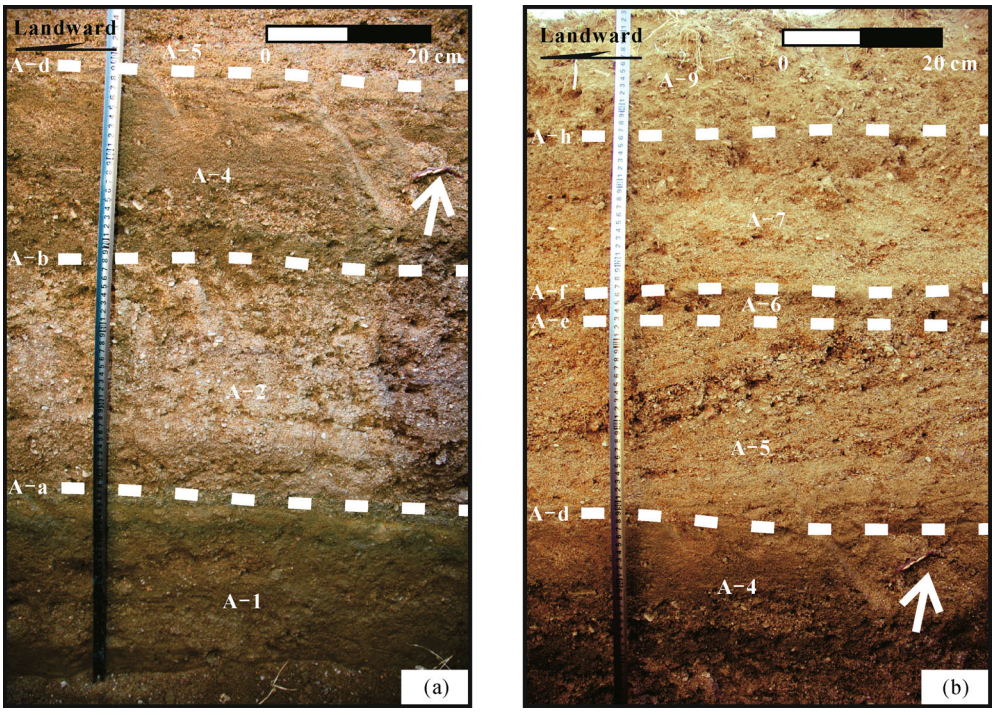

Fig. 3 Trench 1, with interpretation of radar stratigraphy and radar facies on the photo with (a) the lower part of the trench and (b) the upper part. The boundaries (Surfaces A-a, A-b, A-d, A-e, A-f and A-h) and sedimentary units (A-1, A-2, A-4, A-5, A-6, A-7 and A-9) can be correlated well with corresponding radar surfaces and radar facies in Profile A. Sedimentary units A-5 and A-7 display landward-dipping lamination. Note the white arrow which is the same marker in each photograph.

landward, Radar facies B-3 and B-4 are bounded by Surface B-c. Radar facies B-3 is eroded by B-4. Radar facies B-5, B-6 and B-7 are characterized by gently landward dipping, stacked and lenticular sediment sheets. They are interpreted as washover sheet deposits. Radar facies B-8 is interpreted as a soil reworked by eolian processes.

Trench 2 (T2) is showing good correspondence between reflections and surfaces of radar in the GPR profile and sedimentary characteristics of beach ridge in the trench (Fig. 4 and Fig. 5(a)). Boundaries B-a, B-b, B-c, B-d, B-f, and B-g in Trench 2 can be correlated well with the corresponding radar surface in Profile B. Sedimentary units between the surfaces B-a and B-b, B-d and B-f, B-f and B-g correspond to the radar facies B2, B5 and B7 in Profile B and they represent deposits of washover sheets. Sedimentary units between the surfaces B-b and B-c, B-c and B-d correspond to the radar facies B3 and B4 in Profile B and they represent deposits of washover lobes. The sedimentary unit above surface B-g corresponds to radar facies B8 which is immature soil.

4.1.3 Profile C

The beach ridge was imaged by Profile C in a shore-parallel direction along a length of approximately 80 m (Fig. 6). Radar facies C1 is bounded by Surfaces C-a and C-b and has similar reflection characteristics to Radar facies A1. It is interpreted as a beach deposit.

Eight radar packages (C-2 to C-9) overlie radar Surface C-a, and are delineated by Surfaces C-b to C-g (Fig. 6 and Table 3). Radar Surface C-b marks a minor erosional boundary that truncates sub-horizontal reflections in Radar facies C-2. The sediments of Radar facies C-2 to C-8 are interpreted as washover sheet deposits. In the shore-parallel direction, the radar facies of washover origin are characterized by sub-horizontal and middle- high amplitude reflections. Similar internal structures of radar facies and reflection characteristics of washover origin have been described from other beach ridges (Neal et al., 2003). Radar facies C-9 is affected by system noise and is interpreted as representing immature soil containing gravels and in-situ roots.

Trench 3 is in the ESE portion of Profile C. Trench 3 shows a good correspondence between sedimentary stratigraphy and radar facies (Figs. 5(b) and 6). Radar Surfaces C-c, C-f, C-g and C-h are concordant with the surfaces between different lithologies in Trench 3 (Fig. 5 (b)). The sedimentary unit C-2 can be correlated with the corresponding radar facies in Profile C. In sedimentary Unit C-2, the sediments are muddy, medium-grained sand to slightly gravelly medium-coarse grained sand, which shows a coarsening-upward trend. The sedimentary Unit C-2 is overlain by Unit C-5, which is characterized by relatively medium-grained sands, which have a good textural maturity. Unit C-7 is a fining-upward sequence

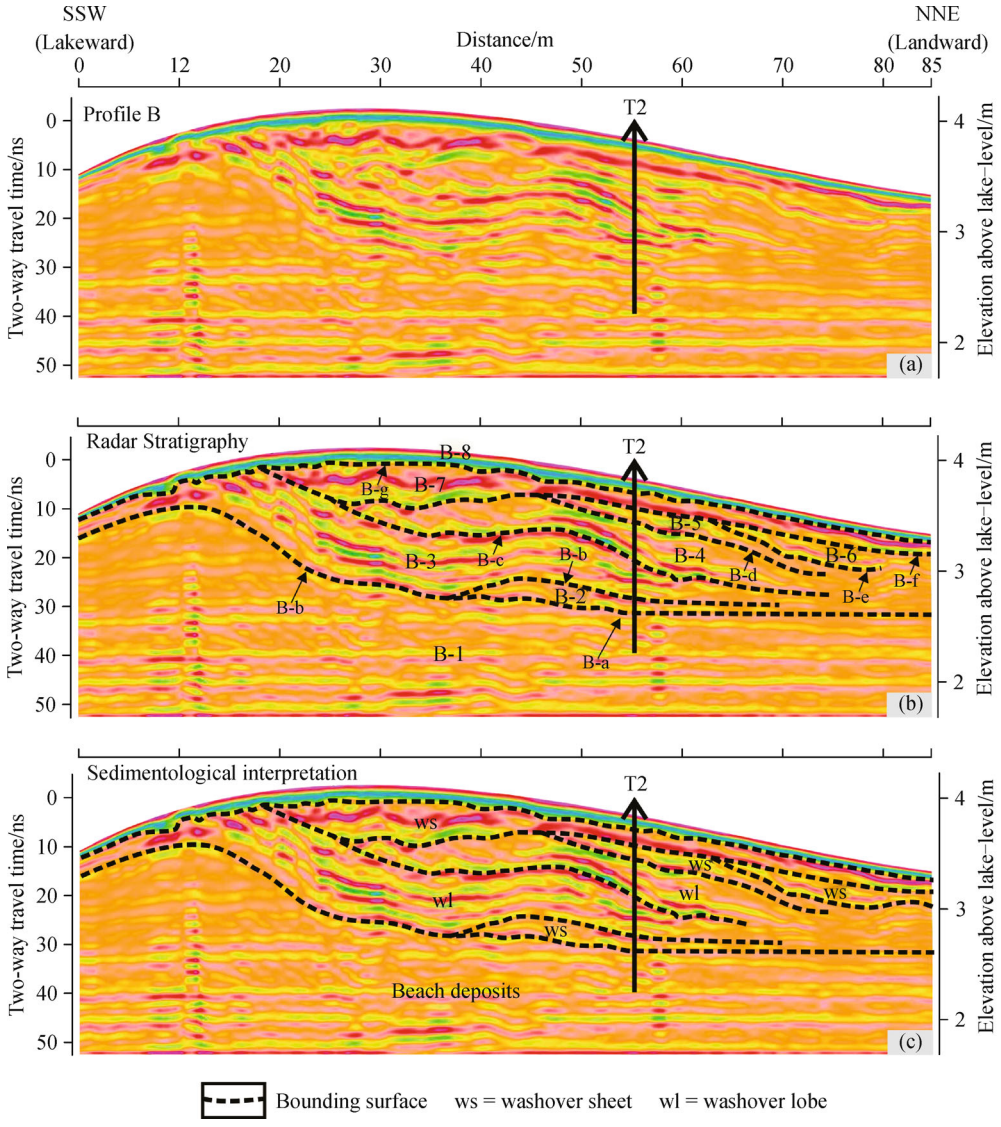

Fig. 4 A 400 MHz GPR survey collected by a TerraSIRch SIR 3000 (Profile B; 85 m length) with (a) the processed GPR profile, (b) the subsurface radar stratigraphy based on the GPR data, and (c) the sedimentological interpretation based on internal reflection characteristics. The dashed lines represent boundaries between different radar facies. ws = washover sheet, wl = washover lobe. T2 shows the location of Trench 2.

Table 2 Characteristics of reflections of different radar facies within Profile B.

RF	Radar surface	Sedimenrary origin	Dip	Continuity	Amplitude
B1	B-a	Beach deposits	Gently landward-dipping	Sub-continuous	Middle
B2	B-a, B-b	Washover sheet	Gently landward-dipping	Discontinuous	High
B3	B-b, B-c	Washover lobe	Steeply landward-dipping	Discontinuous	High
B4	B-c, B-d	Washover lobe	Steeply landward-dipping	Discontinuous	Low-middle
B5	, B-d, B-e	Washover sheet	Gently landward-dipping	Discontinuous	Middle
B6	B-e, B-f	Washover sheet	Landward-dipping	Discontinuous	Middle-high
B7	B-f, B-g	Washover sheet	Gently landward-dipping	Discontinuous	High
B8	B-g	Immature soil	System noise	Continuous	High

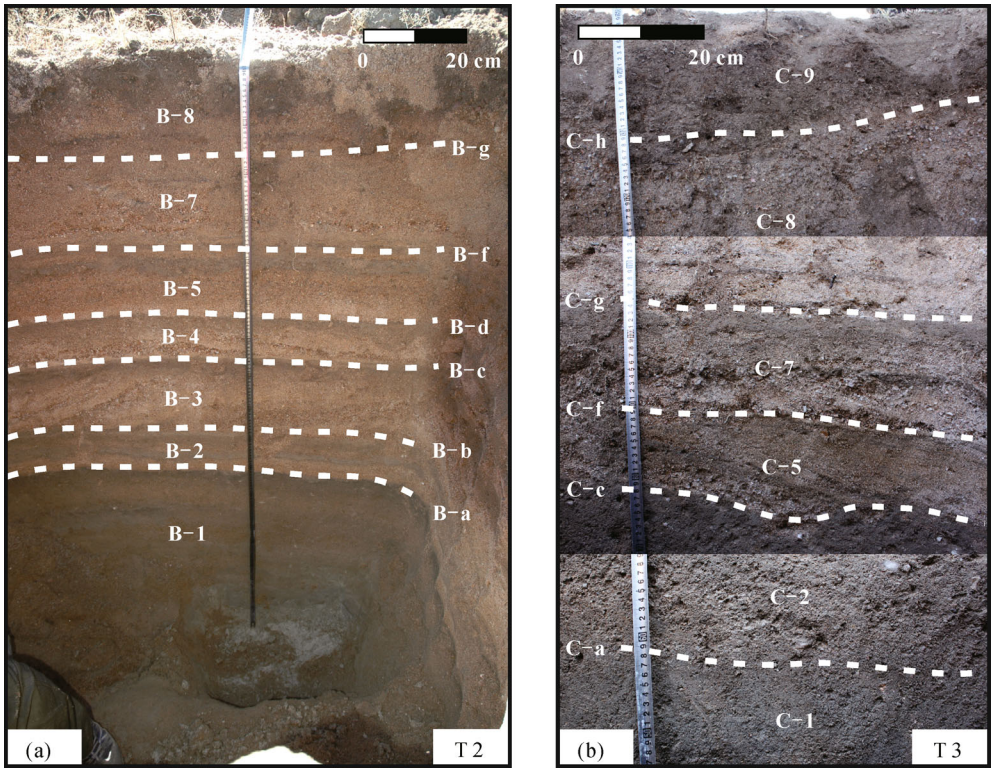

Fig. 5 Trench 2 and Trench 3, with interpretation of radar stratigraphy and radar facies on the photo with (a) Trench 2 with depth of 1.7 m and (b) Trench 3 with depth of 1 m. The boundaries and sedimentary units can be correlated well with corresponding radar surfaces and radar facies in profile B and C.

dominated by moderately gravelly sand. Unit C-7 is overlain by a coarsening-upward sequence, which shows a relatively low textural maturity. Radar facies C-5 and C-7 display gently dipping reflections that parallel the shore and may be influenced by longshore currents. Unit C-9 contains in-situ roots and also other organic fragments and gravels, which together are interpreted as an immature soil.

4.2 Radar facies analysis

Nine kinds of different radar facies were observed in Profiles A, B and C (Fig. 7). The radar facies fall into three groups. The first group consists of facies that display inclined reflections. The second group consists of those that exhibit predominantly horizontal reflections. In the third group, the reflections are irregular.

4.2.1 Radar facies with inclined reflections

Radar facies with inclined reflections and shore-normal directions are interpreted as deposits of washover processes. The landward dipping of moderate to high angle reflections in the GPR profiles are washover lobe clinoforms. Similar radar facies have also been described by Neal et al. (2003). The radar facies with inclined reflections have 4 types.

Radar facies 1-1 show reflections of medium to large amplitude signal that dip at a moderate angle and which are interpreted as washover fan sediments deposited on a moderately inclined topography. These deposits are from the middle part of the washover lobe.

Radar facies 1-2 is characterized by relatively weak to medium reflections with shingled progradation and which are interpreted as prograding washover deposits. This facies is often represented in the distal part of the washover lobe.

Radar facies 1-3 is characterized by large amplitude reflections with a continuous signal and which dip at a moderate angle. This facies is interpreted as deposits from the middle to distal part of the washover lobe.

Radar facies 1-4 is characterized by large amplitude, discontinuous reflections with a sigmoidal shape and that dip at a high angle. It often represents the deposits in the proximal part of the washover lobe.

4.2.2 Radar facies with horizontal reflections

It is best not to interpret radar facies with horizontal reflections as deposits of specific processes. Radar facies with the horizontal reflections represent deposits formed by different process or a combination of several.

Radar facies 2-1 is typified by medium to high amplitude reflections with a relatively continuous signal. Similar radar facies with horizontal reflections have also been

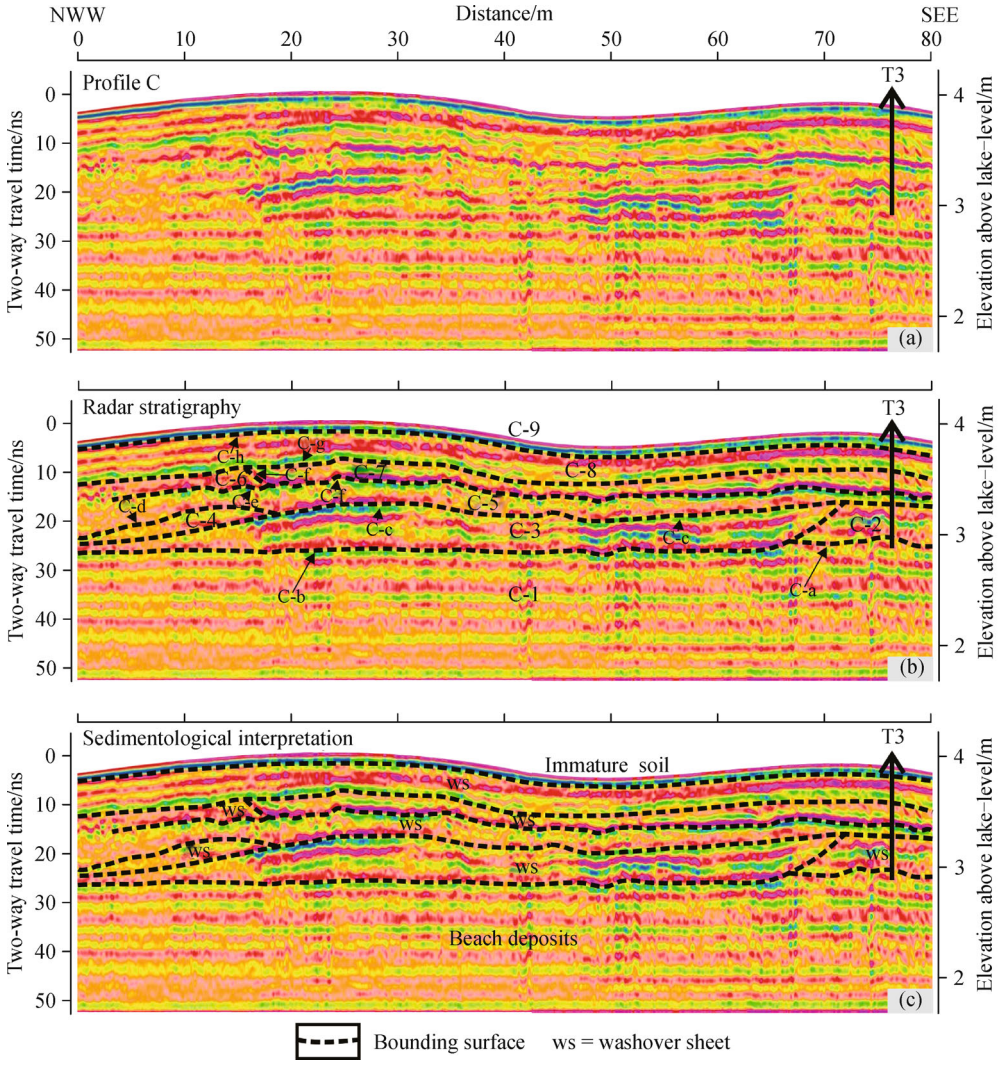

Fig. 6 A 400 MHz GPR survey collected by a TerraSIRch SIR 3000 (Profile C; 80 m length) with (a) the processed GPR profile, (b) the subsurface radar stratigraphy based on the GPR data, and (c) the sedimentological interpretation based on internal reflection characteristics. The dashed lines represent boundaries between different radar facies. ws = washover sheet. T3 shows the location of Trench 3.

Table 3 The characteristic of reflections of different radar facies on Profile C.

RF	Radar surface	Sedimentary origin	Continuity	Amplitude
C1	Ca and C-b	Beach deposits	Continuous	Middle
C2	C-a, C-c	Washover sheet	Discontinuous	Middle-high
C3	C-b, C-c	Washover sheet	Continuous	Middle-high
C4	C-c, C-d	Washover sheet	Discontinuous	Low-middle
C5	C-c, C-d, C-f	Washover sheet	Discontinuous	Middle
C6	C-e , C-g	Washover sheet	Discontinuous	Middle-strong
C7	C-f, C-g	Washover sheet	Discontinuous	Middle-strong
C8	C-g, C-h	Washover sheet	Discontinuous	Middle
C9	C-h	Soil	Continuous	High

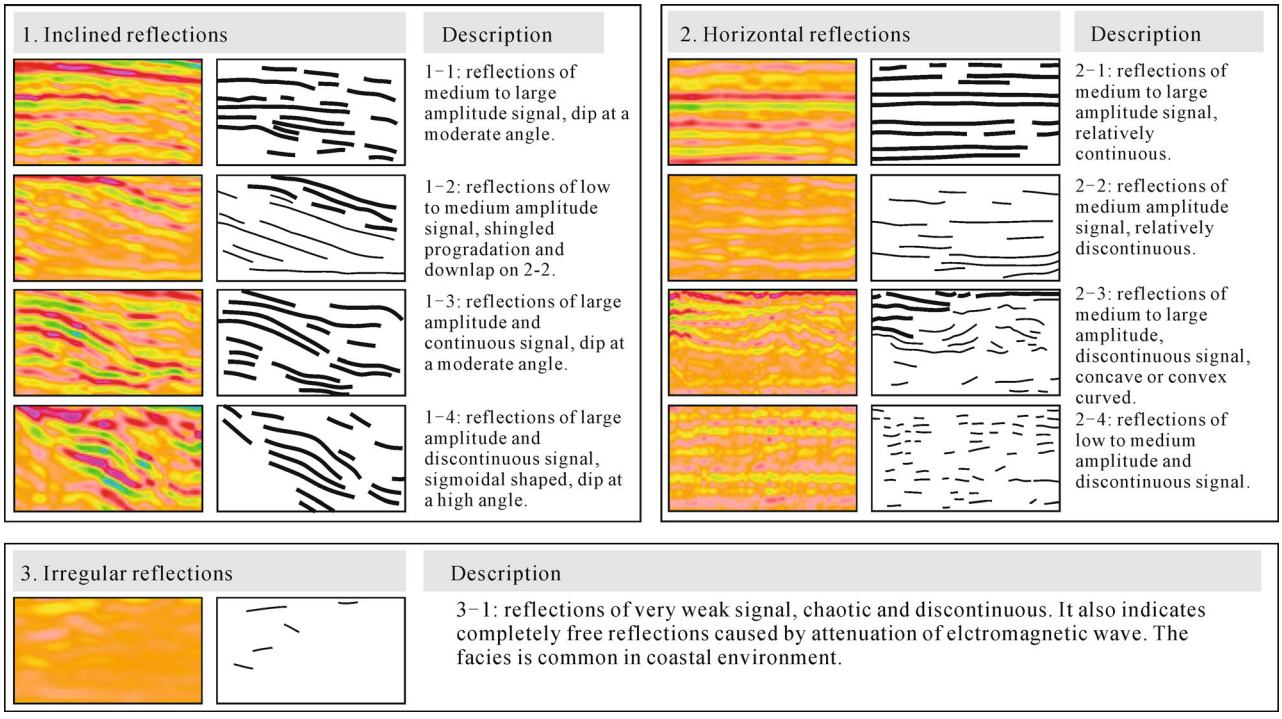

Fig. 7 Radar facies identified in the radar sections. Based on reflection characteristics, the radar facies were divided into three categories: inclined reflections, horizontal reflections and irregular reflections.

described by Nichol (2002).

The characteristics of Radar facies 2-2 are reflections with low to medium amplitude and a discontinuous signal. This represents deposits of relatively homogeneous lithology.

Radar facies 2-3 is characterized by concave-upward radar reflectors that are interpreted as scour and fill boundaries, representing the internal structure of washover channels.

Radar facies 2-4 shows low to medium amplitude reflections and discontinuous signal, which are also interpreted as a form of beach deposit.

4.2.3 Radar facies with irregular reflections

This group represents irregular reflections or reflection-free parts of the GPR profiles. The weak reflections are chaotic and discontinuous. This facies also consists of sections where parts are completely free of reflections as a result of attenuation of the electromagnetic wave. In a marine environment, this often indicates saltmarsh peat deposits or salt water intrusion in the subsurface. Although massive homogeneous lithologic units also lead to reflectionless images, most of the cases are caused by the occurrence of peat or salt water intrusion. There were no occurrences of large amplitude, discontinuous, oblique chaotic reflections, such as those described by Sebastian et al. (2008), which represent sediments deposited on high gradient topography. These facies are common near the coastline where saline lake water and lagoonal marsh are present. The salt marsh is always below the beach-ridge deposits.

5 Discussion

The radar surfaces are interpreted as either the product of sediment bypass or minor erosion. Radar facies with different reflections bounded by radar surfaces are interpreted as bedding or lamination formed by washover or wave processes. Radar facies with gently landward dipping reflections in the shore-normal profile are interpreted as washover sheet deposits. Radar facies with steeply landward-dipping and imbricated reflections are interpreted as washover lobes. In contrast, radar facies with lakeward-dipping reflection patterns are interpreted as representing swash lamination formed dominantly by high-energy swash processes. Overall, the GPR profiles indicate that the beach ridge deposits are composed a series of stacked, gently or steeply landward-dipping reflections. The beach-ridge experiences a moderate-high energy wave environment due to its position on the northern shore of Huangqihai Lake. Washover sheets develop when overwash fails to enter a significant body of water and sedimentation takes place entirely on the relatively flattened topography (e.g., beach deposits or earlier washover sheets). Washover lobe development occurs when overwash enters steeply landward dipping topogra-

phy, and sedimentation takes place on the surface of washover sheets or previous washover lobes. The deposits of washover processes (sheets and lobes) are variably truncated and gently downlap onto the underlying marsh peat deposits or older washover deposits.

The beach-ridge deposits are interpreted as having been formed entirely from vertically and laterally stacked washover sheets and washover lobes. They were formed by wave-dominated processes and secondary overwash process. The principal processes responsible for formation of beach ridges are swash flow, supplemented by longshore current. Washovers are generated by overwash when the lake-level is elevated relative to the beach-ridge (Matias et al., 2008). The elevation of the lake-level is often induced by events such as onshore winds or storm waves (Morton et al., 2000). Overwash is a process in which swash excursions manage to cross the crest of subaqueous dunes. Washover represents an increased volume of overwashing process driven by local morphologic and lacustrine conditions. The frequency and magnitude of washover is controlled by beach topography and climate conditions. In fair-weather conditions, lake-level would be rising and washover would begin carrying material landward. The water level on the lake side of the beach ridge would run up and the wave would carry over beach ridge crest. This would result in washover-sheet development. In storm-weather conditions, washover sheet deposits would be replaced by washover lobe deposits. As lake level continued to rise to its maximum level, the competent and unidirectional flow would carry increased volumes of material at a high speed.

6 Conclusions

The GPR data were used to analyze the beach ridge system on the north shore of Huangqihai Lake. The primary conclusions of this study can be summarized as follows:

1) The identified radar facies can be assigned into three groups (inclined, horizontal and irregular groups) based on the nature of the internal reflections. In the irregular group, the reflections are weak.

2) Radar facies with reflections that dip gently landward in the shore-normal profiles are interpreted as washover sheet deposits. Radar facies with steeply landward-dipping and imbricated reflections are interpreted as washover lobes. Washover sheets develop when overwash fails to enter a significant body of water and sedimentation takes place entirely on the relatively flattened topography (e.g., beach deposits or previous washover sheets). Washover lobes development occurs when overwash enters a zone with topography dipping steeply landward, and where sedimentation takes place on the surface of washover sheets or older washover lobes.

3) The beach-ridge deposits are interpreted as being formed entirely from vertically and laterally stacked washover sheets and washover lobes. They were formed by wave-dominated processes and secondary overwash processes.

Acknowledgements This paper was supported by the State Scholarship Fund (Grant No. 201406400030), the National Natural Science Foundation of China (Grant No. 41072084) and Research Fund for the Doctoral Program of Higher Education (Grant No. 20120022130002). The authors sincerely thank Professor Lars B. Clemmensen of University of Copenhagen for his constructive idea. The authors also thank Beibei Liu, Yonghui Du, Zhaopu Gao and Yanan Miao for their assistance in the field and laboratory. Clift thanks the Charles T. McCord Chair in Petroleum Geology for support. The authors also thank two anonymous reviewers.

References

Anthony E J (1995). Beach-ridge development and sediment supply: examples from West Africa. Mar Geol, 129(1–2): 175–186

Bennett M R, Cassidy N J, Pile J (2009). Internal structure of a barrier beach as revealed by ground penetrating radar (GPR): Chesil beach, UK. Geomorphology, 104(3–4): 218–229

Best J L, Ashworth P J, Bristow C S, Roden J (2003). Three-dimensional sedimentary architecture of a large, mid-channel sand braid bar, Jamuna River, Bangladesh. J Sediment Res, 73(4): 516–530

Bristow C (2009). Ground penetrating radar in Aeolian dune sands. In: Harry M J, ed. Ground Penetrating Radar Theory and Applications. Amsterdam: Elsevier, 274–295

Corbeanu R M, Soegaard K, Szerbiak R B, John B T, George A M, Wang D M, Steven S, Craig B F, Ari M (2001). Detailed internal architecture of a fuvial channel sandstone determined from outcrop, cores, and 3-D ground-penetrating radar: example from the Middle Cretaceous Ferron Sandstone, East-Central Utah. AAPG Bull, 85: 1583–1608

Deng H W, Xiao Y, Ma L X, Jiang Z L (2011). Genetic type, distribution patterns and controlling factors of beach and bars in the second member of the Shahejie formation in the Dawangbei Sag, Bohai Bay, China. Geol J, 46(4): 380–389

Drake N, Bristow C (2006). Shorelines in the Sahara: geomorphological evidence for an enhanced monsoon from palaeolake Megachad. Holocene, 16(6): 901–911

Harvey N (2006). Holocene coastal evolution: barriers, beach ridges, and tidal flats of South Australia. J Coast Res, 22(1): 90–99

Jiang Z X, Liu H, Zhang S W, Su X, Jiang Z L (2011). Sedimentary characteristics of large-scale lacustrine beach-bars and their formation in the Eocene Boxing Sag of Bohai Bay Basin, East China. Sedimentology, 58(5): 1087–1112

Jol H M, Bristow C S (2003). GPR in sediments: advice on data collection, basic processing and interpretation, a good practice guide. In: Bristow C S, Jol H M, eds. Ground Penetrating Radar in Sediments. Geol Soc London Spec Publ, 211: 9–27

Lee K, Gani M R, McMechan G A, Bhattacharya J P, Nyman S L, Zeng X (2007). Three-dimensional facies architecture and three-dimensional calcite concretion distributions in a tide-influenced delta front, Wall Creek Member, Frontier Formation, Wyoming. AAPG Bull, 91 (2): 191–214

Leeder M (2011). Sedimentology and Sedimentary Basins: from

Turbulence to Tectonics (2nd ed). Oxford: Wiley-Blackwell, 319–343

Matias A, Ferreira Ó, Vila-Concejo A, Garcia T, Dias J A (2008). Classification of washover dynamics in barrier islands. Geomorphology, 97(3–4): 655–674

Miall A D (1988). Architectural elements and bounding surfaces in fluvial deposits: anatomy of the Kayenta Formation (Lower Jurassic), Southwest Colorado. Sediment Geol, 55(3–4): 233–262

Morton R A, Gonzalez J L, Lopez G I, Correa I D (2000). Frequent non-storm washover of barrier islands, Pacific Coast of Colombia. J Coast Res, 16(1): 82–87

Neal A (2004). Ground-penetrating radar and its use in sedimentology: principles, problems and progress. Earth Sci Rev, 66(3–4): 261–330

Neal A, Pontee N I, Pye K, Richards J (2002). Internal structure of mixed-sand-and-gravel beach deposits revealed using ground-penetrating radar. Sedimentology, 49(4): 789–804

Neal A, Richards J, Pye K (2003). Sedimentology of coarse-clastic beach-ridge deposits, Essex, southeast England. Sediment Geol, 162 (3–4): 167–198

Nichol S L (2002). Morphology, stratigraphy and origin of last intergacial beach ridges at bream bay, New Zealand. J Coast Res, 18: 149–159

Nichols G (2009). Sedimentology and Stratigraphy. Oxford: Wiley-Blackwell, 151–161

Nielsen L, Clemmensen L B (2009). Sea-level markers identified in ground-penetrating radar data collected across a modern beach ridge system in a microtidal regime. Terra Nova, 21(6): 474–479

Otvos E G (2000). Beach ridges—Definitions and significance. Geomorphology, 32(1–2): 83–108

Scholz C A, Rosendahl B R, Scott D L (1990). Development of coarse-grained facies in lacustrine rift basins: examples from East Africa. Geology, 18(2): 140–144

Sebastian L, Christian B, Christian H (2008). The sedimentary architecture of a Holocene barrier spit (Sylt, German Bight): swash-bar accretion and storm erosion. Sedimentary geolology, 206: 1–16

Talbot M R, Allen P A (1996). Lakes. In: Reading H G, ed. Sedimentary Environments: Processes, Facies and Stratigraphy. Oxford: Blackwell, 89–91

Tamura T, Murakami F, Nanayama F, Watanabe K, Saito Y (2008). Ground-penetrating radar profiles of Holocene raised-beach deposits in the Kujukuri strand plain, Pacific coast of eastern Japan. Mar Geol, 248(1–2): 11–27

Yu X H, Li S L, Chen B T, Tan C P, Xie J, Hu X N (2012). Interaction between downslope and along slope processes on the margins of Daihai Lake, North China: implication for deltaic sedimentation models of lacustrine rift basin. Acta Geol Sin, 86(4): 932–948

Zhang J R, Jia Y L, Lai Z P, Long H, Yang L H (2011). Holocene evolution of Huangqihai Lake in semi-arid northern China based on sedimentology and luminescence dating. Holocene, 21(8): 1261–1268